Article

Not peer-reviewed version

Drying of Cirina Forda Caterpillar: Experiments and Modeling

Célestin Bukamba Tshanga , Charlotte Van Engeland , Myriam Kapuku Kayiba , Bienvenu Kambashi Mutiaka , Jérôme Bindelle , Benoit Haut * , Frédéric Debaste

Posted Date: 23 May 2024

doi: 10.20944/preprints202405.1478.v1

Keywords: Solar drying; Cirina Forda; Drying kinetics; Shrinkage; Diffusion

 doi:10.20944/preprints202405.1478.v1

Article

Drying of Cirina Forda Caterpillar: Experiments and Modeling

Célestin Bukamba Tshanga [1,2,*], Charlotte Van Engeland [1], Myriam Kapuku Kayiba [2], Bienvenu Kambashi Mutiaka [3], Jérôme Bindelle [4], Benoît Haut [1] and Frédéric Debaste [1]

[1] Université libre de Bruxelles (ULB), Transfers, Interfaces and Processes (TIPs), Avenue F.D. Roosevelt, 50 CP165/67, 1050 Bruxelles, Belgique
[2] Université de Kinshasa, Faculté des Sciences Agronomiques, Département de chimie et industries agricoles, Route Kimwenza N°1, Kinshasa, DR Congo
[3] Université de Kinshasa, Faculté des Sciences Agronomiques, Département de Zootechnie, Route Kimwenza N°1, Kinshasa, DR Congo
[4] University of Liège, Gembloux Agro-Bio Tech, Terra AgricultureIsLife, Passage des Déportés 2, B-5030, Gembloux, Belgium
* Correspondence: celestin.bukamba.tshanga@ulb.be

Abstract: *Cirina forda* caterpillars are a significant protein source in Central Africa, yet their preservation and consumption pose challenges. This study investigates the drying of *Cirina forda* caterpillars to enhance preservation methods and product quality. Caterpillars were subjected to drying experiments at temperatures ranging from 40°C to 70°C, using tunnel and oven dryers. The drying kinetics was analyzed using mathematical models, revealing a water diffusion-limited mechanism in all the tested conditions. The Newton model provided adequate estimations of the drying behavior, facilitating further practical dryer design. Shrinkage analysis indicated a two-step process independent of the drying conditions. Achieving a moisture content suitable for prolonged storage resulted in substantial volume loss, highlighting the challenges of preserving dried caterpillars. These findings shed light on how to optimize drying processes for *Cirina forda* caterpillars, crucial for sustaining protein sources in Central Africa.

Keywords: solar drying; cirina forda; drying kinetics; shrinkage; diffusion

1. Introduction

Insects are consumed since the prehistoric period and around 2000 insect species are globally consumed nowadays, principally Coleoptera (31%), Lepidoptera (18%), Hymenoptera (14%), Orthoptera (13%), and Hemiptera (10%). These are consumed by 2 billion people, in particular in Asia, Africa and Latin America [1]. Insects are consumed at distinct life stages: eggs, larvae, pupae or adults [2]. With a low demand for land, water and a better feed conversion than traditional farmed animals, insects provide a large amount of suitable energy, fat, and protein [3–5]. The growth in world population is causing an increase in the global demand for food, in particular of proteins sources, mainly in developing countries [5]. In 2050, the global human population is predicted to reach 9 billion. In this regard, edible insects present a sustainable protein source [5,6].

The literature reports that dead insects can undergo some processing for their preservation or consumption, such as drying, toasting, frying, roasting or boiling [7–10]. Drying makes seasonal insects available all year round. Sun drying is the most common process applied to the edible insects in Africa after their collection in the wild [10]. This drying is mostly based on purely empirical habits. Yet, the drying conditions have an impact on the quality of the final product. Some research showed that the processing method affects the nutritional potential of edible insects by changing the nutriment proportions, protein digestibility, and the amino acid and vitamin content [8,9,11,12]. Moreover, the process of the drying can induce a shrinkage of the product, that can have an impact on the drying dynamics as well as on the final product properties (size, shape, porosity...) [13].

The knowledge of the characteristics of the drying of a given product allows the design and the control of an efficient process, leading to an enhanced and more reproducible final product. In recent years, there has been an abundance of scientific production on edible insects but very little on

 doi:10.20944/preprints202405.1478.v1

the characterization of their drying [9,14] and even less on the shrinkage dynamics. Loss of water and heating during drying can cause volume reduction of foodstuffs, due to important stresses in the cellular structure leading to change in shape and decrease in dimensions [15]. The parameters controlling this shrinkage are not correctly identified for insects. Yet, this shrinkage can both impact the kinetics and the final product acceptance by the consumer [16].

Consequently, there is a lack of information on the drying of many edible insects, such as *Cirina forda*. However, *Cirina forda* caterpillars are one of the most consumed caterpillars in Central Africa. Traditionally, the caterpillars are dried in the open air under direct solar irradiation. This method has several disadvantages for food products, such as uncertain drying time, high labor cost, the need for large areas, risk of infection by insects or microorganisms, presence of other foreign bodies, etc. All these can cause a poor quality of the final product [17] and a reduced guarantee of revenue for the producer. To overcome these problems, it is necessary to develop dryers that ensure a better control of the process and, thus, of the product quality [18]. Designing a dryer requires mastering the drying characteristics of the product of interest.

Therefore, the aim of this work is to provide and understand the characteristics of *Cirina forda* drying by measuring the drying kinetics and the evolution of the size of *Cirina forda* caterpillars over time. Simple mathematical models based on strong physical assumptions are used to simulate the experimental behavior and propose first basic explanations of the phenomena controlling the drying kinetics of these caterpillars. To propose such a first explanation, a follow up of the size of the insects at different stages of the drying is realized.

2. Materials and Methods

2.1. Material: Cirina Forda Caterpillars

Living caterpillars were purchased from the market in Kinshasa, Democratic Republic of Congo. They were packed in sealed plastic bags and stored at -20°C until use. Just before use, the caterpillars were left overnight to thaw at room temperature.

2.2. Measurement of the Dry Matter Content

In parallel with each drying experiment (see below), the dry matter content of the caterpillars was evaluated by the oven method at 105°C. A sample with an initial mass M_0 of around 6 g was placed in an oven at 105°C and weighed every 24h until a constant mass M_f was obtained.

The initial moisture content of the sample X_0, expressed in a dry basis (kg of water per kg of dry matter), was calculated by:

$$X_0 = \frac{M_0 - M_f}{M_f} \tag{1}$$

This analysis was done in triplicate.

2.3. Drying Experiments

Drying experiments of caterpillars were carried out in two different set-ups:

1. a tunnel dryer developed by Spreutels *et al.* [13]. This device allows a drying with well-controlled local conditions and an in situ mass measurement. However, this device is limited to a maximal drying temperature of 60°C.
2. an oven dryer with less controlled conditions and manual mass measurement that requires to take the sample out of the drying chamber for each measurement but that allows temperature above 60 °C. This set-up is used to extend the tested conditions to 70°C.

In the tunnel dryer, a fan generates an air flow of 20 $Nm^3.h^{-1}$, corresponding to an air velocity of approximately 0.5 $m.s^{-1}$ around the sample. This air flow is brought to the desired temperature by a heating resistance controlled by a regulator coupled to a thermocouple. The air enters the tunnel to

 doi:10.20944/preprints202405.1478.v1

dry the sample that is placed on a plate connected to a Sartorius ENTRIS22021-1S weighing balance. This balance measures and records the mass of the sample every 10 minutes. A multimeter Testo 400 records the humidity and the temperature of the air a few centimeters downstream of the sample during the drying. For each experiment, a sample of three caterpillars (around 6 g) was placed on the balance. They were dried at a constant temperature during the whole experiment. Tests were realized at 40, 50 and 60°C. The sample was allowed to dry until no significant loss of its mass was recorded for at least 30 minutes. By night, tests were interrupted. Samples were sealed in aluminium and placed a dessicator overnight. Each drying condition was tested in duplicate.

For the tests in the oven dryer, a sample of around 30 g of caterpillars was placed in an oven on a tared support. The sample was weighed after every hour. Tests were realized at 60 and 70°C. The sample was allowed to dry until no significant loss of its mass was recorded for at least 2 hours. Each drying condition was tested in duplicate. Complementary tests for shrinkage measurements (without kinetics analysis) were also performed in duplicates at 50°C.

2.4. Moisture Content, Moisture Ratio and Drying Rate Calculations

For each drying experiment, the moisture content of the sample at time t, written X_t, expressed in dry basis (kg of water per kg of dry mater), was calculated based on its measured mass at time t, written M_t, and on the value of X_0 determined in parallel by the oven method:

$$X_t = \frac{M_t(1+X_0)}{M_{t=0}} - 1 \tag{2}$$

The moisture ratio of the sample at time t, written MR_t, was calculated as:

$$MR_t = \frac{X_t - X_{\text{eq}}}{X_0 - X_{\text{eq}}} \tag{3}$$

where X_{eq} is the moisture content of the sample at the end of the drying (i.e., when equilibrium is reached between the sample and the drying air).

The drying rate $J_t = -dX_t/dt$ (in kg of water evaporated per unit of time and per kg of dry mater in the sample) was estimated using the Savitzky-Golay method for the first derivative, with a window size depending on the considered time step summarized in Table 1 [19].

Table 1. Savitzky-Golay method for the first derivative used to estimate the evaporation rate J with Δt is the time interval between two measurements (10 minutes for the tunnel dryer and 1h for the oven dryer).

Time step	**Windows size**	**Equation $J_t =$**
First and last	None	0
Second and second-to-last	3	$\frac{1}{\Delta t}(-X_{t-\Delta t} + X_{t+\Delta t})$
Third and third-to-last	5	$\frac{1}{12\Delta t}(-X_{t-2\Delta t} + 8X_{t-\Delta t} - 8X_{t+\Delta t} + X_{t+2\Delta t})$
Forth and forth-to-last	7	$\frac{1}{252\Delta t}(-22X_{t-3\Delta t} + 67X_{t-2\Delta t} + 58X_{t-\Delta t} - 58X_{t+\Delta t} - 67X_{t+2\Delta t} + 22X_{t+3\Delta t})$
All other time steps	9	$\frac{1}{1188\Delta t}(-86X_{t-4\Delta t} + 142X_{t-3\Delta t} + 193X_{t-2\Delta t} + 126X_{t-\Delta t} - 126X_{t+\Delta t} - 193X_{t+2\Delta t} - 142X_{t+3\Delta t} + 86X_{t+4\Delta t})$

 doi:10.20944/preprints202405.1478.v1

2.5. Modeling of the Drying Kinetics

Three different classical thin layer drying models were tested against the experimental results. Two of them, giving the most relevant results and interpretation, are presented here. The third on (Page model) is presented and shortly discussed in appendix B.

The first and simplest model of this category is the Newton model. It is based on the assumption that the evaporation rate is directly proportional to the water content:

$$\frac{dX_t}{dt} = -J_t = -kX_t \tag{4}$$

where k (s^{-1}) is a kinetic constant, sole parameter describing the global timescale of the drying. Integrating equation 4 gives:

$$MR_t = \exp(-kt) \tag{5}$$

The second model is a variation of the Newton model, the Henderson and Pabis model [20]. This model generalizes equation 5 by multiplying the righthand side by a dimensionless constant a:

$$MR_t = a\exp(-kt) \tag{6}$$

The physical interpretation of the Henderson and Pabis is limited. Nevertheless, such an expression of the moisture ratio over time can be obtained when solving an equation describing the diffusion of water in a porous slab of thickness H_0, with an effective diffusion coefficient D_{eff} ($m^2.s^{-1}$), and keeping only the first term of the series giving the exact solution of the equation, yielding [21]:

$$MR_t = \frac{8}{\pi^2}\exp\left(-\frac{4\pi^2 D_{\text{eff}}}{H_0^2}t\right). \tag{7}$$

The error induced by neglecting the further terms of the series when compared to the exact solution of the diffusion equation is below 1% when $t > 0.123H_0^2/(4D_{\text{eff}})$.

Expressing the model as a diffusion one allows further physical interpretation. In particular, the influence of the temperature on the effective diffusion coefficient can often be expressed following an empirical Arrhenius law:

$$D_{\text{eff}} = D_0\exp\left(-\frac{E_a}{RT}\right) \tag{8}$$

where E_a is an activation energy ($J.mol^{-1}$), D_0 is a pre-exponential factor ($m^2.s^{-1}$), R is the ideal gaz constant (8.314 $J.mol^{-1}.K^{-1}$) and T the drying temperature (K).

2.6. Shrinkage Measurement

The length L, width W, and thickness H (all in mm) of the caterpillars at different stages of their drying were measured using a digital caliper (Figure 1). The distance from the tip of the head to the tail was taken as the length. Positioning the caterpillar with its feet on a horizontal surface, the width and thickness are respectively defined as the horizontal and vertical sizes of the caterpillar in the plan perpendicular to the length (see Figure 1). W and H were estimated based on the average of measurements at the head, mid-body and tail of the caterpillar. 30 fresh caterpillars were measured to characterize their geometry. For dried samples, 10 insects randomly selected were monitored during their drying in the oven, and average values of L, W and H were determined at different drying times. The volume V of a caterpillar was estimated by taking the product of the three measured dimensions:

$$V = LWH \tag{9}$$

 doi:10.20944/preprints202405.1478.v1

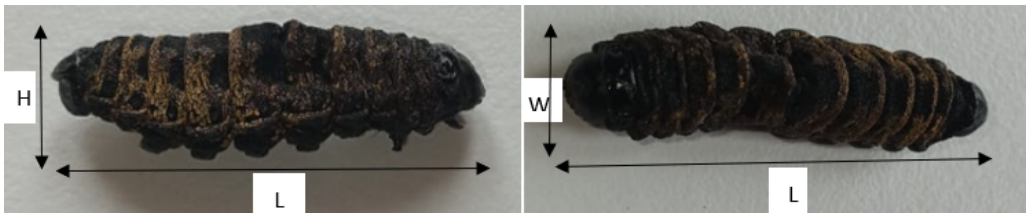

Figure 1. Dimensions of *Cirina Forda* caterpillar. Left is the side view. Right is the top view.

2.7. Modeling of the Shrinkage

Shrinkage during air-drying is typically illustrated by plotting the dimensionless volume ratio (V_t/V_0) (i.e., the ratio between the volume at time t and the initial volume) as a function of the moisture ratio MR.

If the volume of solid is constant over time and if the fluid volume (initially assumed to be fully composed of water) decreases monotonically during the drying with a constant fraction α of the volume of the evaporated liquid yielding a volume of gas staying inside the sample, the link between the volume ratio and the moisture ratio writes (see appendix C):

$$\frac{V_t}{V_0} = 1 - \epsilon_0(1-\alpha)(1-MR_t) \tag{10}$$

where ϵ_0 is the initial porosity of the sample, estimated as the initial volume of water in the sample divided by the initial total volume of the sample.

The porosity ϵ_t of the sample at time t is the fraction of the total volume of the sample that is occupied by fluid (gas and liquid). Following the same assumptions as for the evolution of the volume ratio with the moisture ratio, the porosity as a function of the moisture ratio writes (see appendix C):

$$\epsilon_t = \epsilon_0 \frac{\alpha + (1-\alpha)MR_t}{1 - \epsilon_0(1-\alpha)(1-MR_t)} \tag{11}$$

If a linear relationship between MR_t and V_t/V_0 is indeed observed experimentally, equation (10) indicates that the slope of the line is $\epsilon_0(1-\alpha)$, while its value at $MR_t = 0$ is equal to $1-\epsilon_0(1-\alpha)$, so that their sum should be equal to 1. Knowing the initial values of the volume, mass, and water content of a sample, an estimate of ϵ_0 can be calculated and a value of α can be further deduced. Equation (11) can then be used to estimate the evolution of the porosity of the sample as a function of MR_t.

2.8. Fitting of the Models

The k parameter appearing in equations (5) of the Newton model and (6) of the Henderson and Pabis model (with a fixed at a value of $8/\pi^2$) were obtained, for each drying experiment, by a linear least-square fitting of $\ln(MR_t)$ as a function of t. To limit the impact on the fitting quality of the high relative error on the experimental values of MR_t at low moisture content, only data for $MR_t > 0.2$ were taken into consideration for the fitting.

Both coefficient of correlation (r^2) and the root mean square error analysis ($RMSE$) were used to evaluate the quality of the fitting [14]:

$$r^2 = \frac{\sum_{i=1}^{N}\left(MR_{pre,i} - \overline{MR}_{exp}\right)^2}{\sum_{i=1}^{N}\left(MR_{exp,i} - \overline{MR}_{exp}\right)^2} \tag{12}$$

$$RMSE = \sqrt{\frac{\sum_{i=1}^{N}\left(MR_{pre,i} - MR_{exp,i}\right)^2}{N-p}} \tag{13}$$

 doi:10.20944/preprints202405.1478.v1

where $MR_{pre,i}$ is the predicted value of MR_t at time i, $MR_{exp,i}$ is the measured value of MR_t at time i, $\overline{MR}_{exp}$ is the average of the experimental values of MR_t, N is the number of values and p is the number of adjusted parameters. The statistical analysis was done with Excel 2010 and Matlab R2023a.

Using the Henderson and Pabis model, the value of the effective diffusion coefficient D_{eff} can be deduced for each experiment from the value of k, knowing the initial thickness H_0 of the caterpillars. Then, the activation energy E_a can be estimated by a linear least-square fitting of the plot of $\log(D_{\text{eff}})$ as a function of T^{-1} (see equation 8).

3. Results

3.1. Initial Sample Properties

Cirina forda dimensions and water content prior to drying are presented in Table 2.

Table 2. Initial dimensions and water content of *Cirina forda* larvaes based on 30 initial samples).

Property	Average	Standard deviation
Length L_0 (mm)	43.3	4.9
Width W_0 (mm)	6.11	0.73
Thickness H_0 (mm)	6.04	0.81
Volume V_0 (mm^3)	1612	610
Moisture content X_0 ($kg_{water}kg^{-1}_{drymater}$)	3.35	0.19

3.2. Drying Curves

Figure 2 (left) presents the experimental drying curves with the evolution of the moisture ratio as a function of the time, for the different drying temperatures, while Figure 2 (right) presents the drying rate J_t as a function of the water content X_t of the sample. For the test at $40°C$ in the tunnel dryer, the total duration of the drying is of 60h. The last 30h are not shown on Figure 2 (left) for clarity of the figure.

At $60°C$, both the oven and the tunnel dryers were tested. We see in Figure 2 that they show similar results although the oven gives a slightly faster drying during the second half of the drying, leading to the prediction of a 12% shorter total drying time. This difference is mostly attributed to the lower control of the local conditions inside of the oven compared to the control in the tunnel. We can nevertheless conclude that it is relevant to group all the drying results, at the different temperatures, on a same figure.

Figure 2 (right) shows that, in all the tested conditions, the drying of *Cirina forda* caterpillars is characterized by the absence of a constant rate period, as J_t monotonically decreases with a decrease of X_t. Therefore, we can assume that this drying is controlled by internal transport mechanisms, rather than external ones. This was also observed for many food products, including some insects, such as yellow mealworm [14].

 doi:10.20944/preprints202405.1478.v1

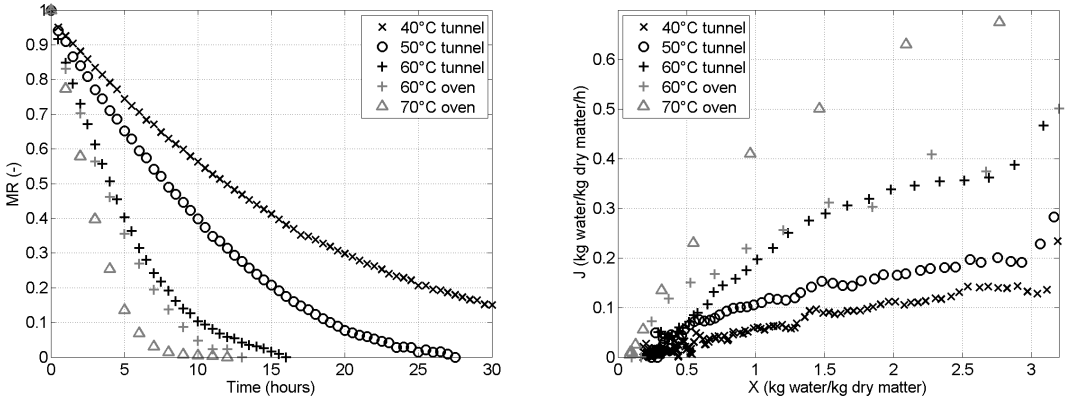

Figure 2. Black symbols correspond to tests in the tunnel dryer while gray symbols correspond to tests in the oven dryer. Each symbol corresponds to a given drying temperature. (left) Moisture ratio MR_t as a function of time. (right) Drying rate J_t as a function of the solid water content X_t.

3.3. Modeling of the Drying Kinetics

Table 3 presents the identified value of k for both the Newton and the Henderson and Pabis models, with a pre-exponential factor fixed to $8/\pi^2$ for the latter, along with the corresponding r^2 and $RMSE$. The Newton model offers, in all the tested conditions, a better fitting, with a good level of accuracy (lowest r^2 at 0.979 and maximum $RMSE$ at 0.055). Appendix B also present the results obtained with the two adjustable parameter Page empirical models. The gain of offering a second degree freedom in parameter adjustment is marginal as the r^2 are only slightly higher. In Appendix A, Figure A1 illustrates the fitting obtained with the Newton model.

The good quality of the fitting with both the Newton and the Henderson and Pabis models highlights that, in all the tested conditions, the drying seems to be limited by the same, diffusion like, set of transport phenomena, with some minor effects inducing a deviation from the analytical solution of the diffusion equation. Possible effects might, for example, be shrinkage and/or deformation of the insects during their drying.

As expected when looking at the drying curves in Figure 2 (left), the value of k significantly increases with the temperature.

 doi:10.20944/preprints202405.1478.v1

Table 3. Identified values of k (with $a = 8/\pi^2$ for the Henderson and Pabis model) and the corresponding statistics for the two tested models at different temperatures.

Experiments	Parameter	Newton	Henderson and Pabis
40°C in tunnel	$k\ (h^{-1})$	3.7	4.4
	r^2	0.998	0.968
	$RMSE$	0.021	0.099
50°C in tunnel	$k\ (h^{-1})$	5.8	7.0
	r^2	0.985	0.971
	$RMSE$	0.055	0.091
60°C in tunnel	$k\ (h^{-1})$	11.7	13.8
	r^2	0.987	0.974
	$RMSE$	0.050	0.089
60°C in oven	$k\ (h^{-1})$	12.3	15.2
	r^2	0.988	0.963
	$RMSE$	0.049	0.107
70°C in oven	$k\ (h^{-1})$	19.2	23.4
	r^2	0.979	0.967
	$RMSE$	0.075	0.115

3.4. Effective Diffusion Coefficient and Activation Energy

As mentioned previously, the values of the effective diffusion coefficient D_{eff} were deduced from the values of k obtained using the Henderson and Pabis model, knowing the initial thickness H_0 of the caterpillars. Figure 3 gives the value of the logarithm of D_{eff} as a function of the inverse of the product of the temperature T and the ideal gas constant R. The good quality ($r^2 = 0.988$) of the linear fitting observed, the slope of which is the opposite of the activation energy E_a (see equation 8), confirms an Arrhenius like behavior of the dependence of D_{eff} on T, for the tested range of temperatures.

The calculated values of D_{eff} are between 1.15 10^{-9} $m^2.s^{-1}$ (at 40°C) and 6.14 10^{-9} $m^2.s^{-1}$ (at 70°C). The activation energy E_a and the pre-exponential factor D_0 are evaluated equal to 51.6 $kJ.mol^{-1}$ and 0.457 $m^2.s^{-1}$, respectively.

 doi:10.20944/preprints202405.1478.v1

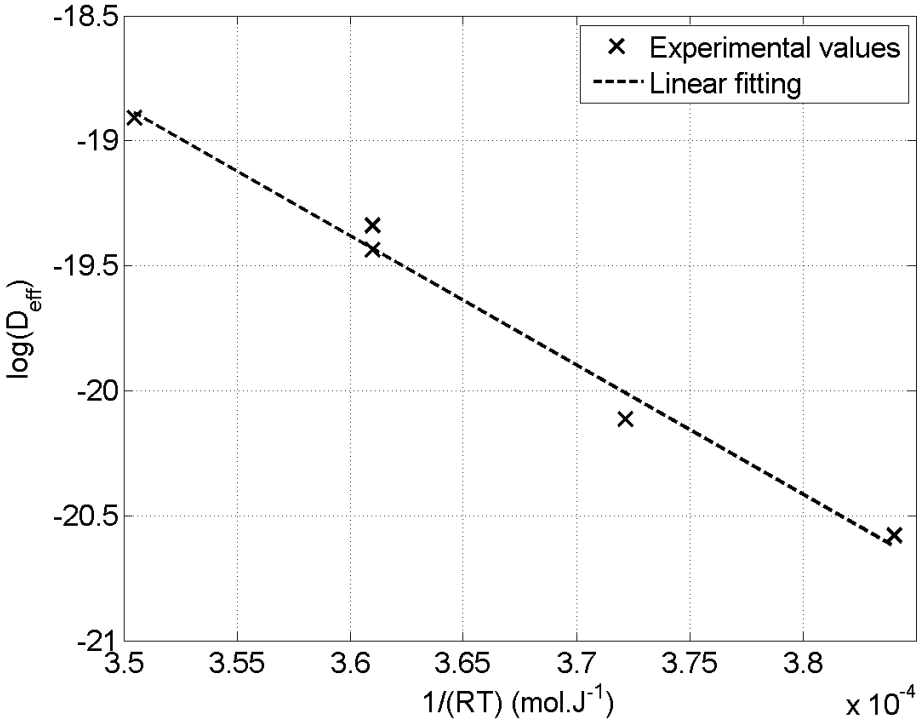

Figure 3. Linear fitting of the logarithm of the effective diffusion coefficient D_{eff} as a function of the inverse of the temperature.

The values of the effective diffusion coefficient and of the activation energy obtained in this work are in the large ranges of values already reported for food products. Indeed, it was reported that the effective diffusion coefficient of most food products is between 10^{-12} and 10^{-6} $m^2.s^{-1}$, while the activation energy is between 12.32 and 406.02 $kJ.mol^{-1}$ [22]. For the specific case of insects, Azzollini *et al.* [14] observed, for yellow mealworm (*Tenebrio molitor*), an effective diffusion coefficient increasing from 4.5 10^{-11} $m^2.s^{-1}$ (at 50°C) to 1.62 10^{-10} $m^2.s^{-1}$ (at 70°C). They obtained an activation energy of 52.1 $kJ.mol^{-1}$ and a pre-exponential factor of 1.38 10^{-2} $m^2.s^{-1}$.

Effective diffusion coefficients (and, accordingly, the pre-exponential factor) for *Cirina forda* appear to be one order of magnitude above the values observed for *Tenebrio molitor* by Azzollini *et al.* [14] while staying in an acceptable range for food product.

On the contrary, the value of the activation energy obtained in this work is really close to the value of Azzollini *et al.* [14] for *Tenebrio molitor* and it is about 20% larger than the latent heat of water vaporization (43 $kJ.mol^{-1}$ at 50°C). Tshanga *et al.* [23] have shown that the isosteric heat of sorption of *Cirina forda* is below 20 $kJ.mol^{-1}$ at 50°C, for a moisture ratio larger than 0.23. Therefore, the observed activation energy could be the expression of the latent heat of vaporisation of water modified by the isosteric heat, leading to the fact that the Arrhenius like behavior corresponds to the thermodynamic Clausius-Clapeyron law for a liquid bound to a solid [24].

This result suggests that the change of the drying rate as a function of the temperature can be mostly attributed to the change of the equilibrium vapor pressure. This confirms that the limiting drying phenomena observed at the different temperatures can be the same and that no other major change in the drying dynamics is observed in this range of temperature.

3.5. Shrinkage and Porosity Evolution

Figure 4 presents the volume ratio as a function of the moisture ratio for three tested temperatures. The three curves follow the same linear trend for $MR_t > 0.07$ while, below that value, the decrease in the volume ratio with a decrease in the moisture ratio is greater. The least-square optimal linear fitting ($r^2 = 0.98$) of the combined set of data for the 3 temperatures and for $MR > 0.07$ is:

 doi:10.20944/preprints202405.1478.v1

$$\frac{V_t}{V_0} = 0.5418\, MR_t + 0.4655 \tag{14}$$

For $MR_t > 0.07$, a value close to 0.54 for the group $\epsilon_0(1-\alpha)$ is thus predicted. Using values of the initial volume, mass and water content of the caterpillars, a initial porosity $\epsilon_0 = 0.77$ can be estimated, leading to a value of $\alpha = 0.3$. In other words, the insect structure collapses progressively as only 30% of the space freed by the evaporated water remains inside of the porous structure. The observed collapse is independent of the temperature, and thus of the kinetics itself.

For $MR_t < 0.07$, the reduction of volume is more pronounced when the moisture ratio decreases and seems also independent of the temperature. The observed change of slope can be interpreted as a rise in the matrix degradation, loosening the mechanical properties of the solid and leading to a more important collapse.

Generally speaking, the results show that the volume of the caterpillars decreases by more than 50% when drying is complete.

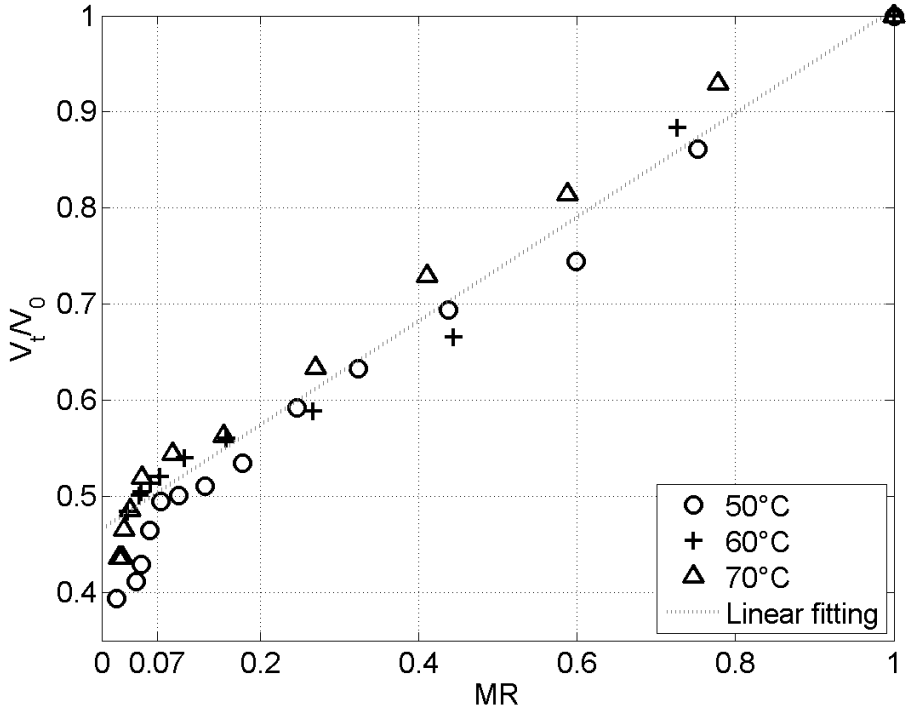

Figure 4. Volume ratio as a function of the moisture ratio for drying at three different temperatures.

4. Discussion and Conclusion

The analysis of the drying behavior of *Cirina forda* in the range of temperature from 40 to 70°C shows results similar to what was observed for many other foodstuffs like banana, potato, apple and carrot [15,25,26]. The drying kinetics globally fits well with a diffusion limited mechanism, with a limiting phenomenon that is the same from the beginning to the end of the drying. The temperature dependence that is observed can be mostly attributed to the change of volatility of water with temperature, including some water bounding effect.

The shrinkage of the product appears to be independent of the temperature, with a two successive steps mechanism. For the first step, corresponding to the majority of the water removal, the water content reduction leads to a partial but regular collapse of the structure. In the second, final shrinking phase, the shrinkage is more pronounced. The two steps of shrinkage cannot be correlated explicitly to a change in the drying rate, as the second shrinkage phase only happens for really low water

 doi:10.20944/preprints202405.1478.v1

content. The impact of the shrinkage on the drying rate is therefore hidden in the fitted value of the k parameter of both the Newton and the Henderson and Pabis models. For further use in the framework of dryer design and optimisation, the Newton model appears to give a sufficient precision, avoiding over-parametrization.

Tshanga *et al.* [23] suggested a conservation moisture content of 8% d.b (0.08 kg/kg) to ensure 12 months of storage in polyethylene bags at 30°C. For the drying of caterpillar with an average initial moisture content $X_0 = 3.35$ kg/kg, such a final value of the water content corresponds to a moisture ratio at the end of the drying equal to 0.024. As mentioned previously, Figure 4 shows that such a final moisture ratio corresponds to a volume reduction of the caterpillars of more than 50%. In other words, this indicates that a direct drying of the caterpillars to a moisture content that guarantees a conservation of one year leads to a loss of almost half of their volume compared to the fresh product.

Author Contributions: Methodology, C.B.T. and F.D.; ; formal analysis, C.B.T and F.D.; investigation, C.B.T., M.K.K. and C.V.E.; resources, F.D. and B.H.; data curation, C.B.T, M.K.K. and F.D.; writing—original draft preparation, C.B.T and F.D.; writing—review and editing, C.V.E., J.B. and B.H.; visualization, C.B.T and F.D.; supervision, F.D.; project administration, B.K.M. and F.D.; funding acquisition, B.K.M., C.V.E., F.D., and J.B. All authors have read and agreed to the published version of the manuscript.

Funding: This research was funded by the Academy for Research and Higher Education (ARES)/ Federation of French-speaking higher education establishments in Belgium/Projet de recherche pour le développement: PRD/Insectes.

Data Availability Statement: The data presented in this study are openly available in [repository name e.g., FigShare] at [doi], reference number [reference number].

Conflicts of Interest: The authors declare no conflict of interest. The funders had no role in the design of the study; in the collection, analyses, or interpretation of data; in the writing of the manuscript; or in the decision to publish the results.

Abbreviations

The following abbreviations are used in this manuscript:

MR	Moisture Ratio
$RMSE$	Root Mean Square Error

Appendix A. Visualisation of the Fitting

Figure A1 compares the experimental time evolution of the MR with the values predicted by the Newton model.

 doi:10.20944/preprints202405.1478.v1

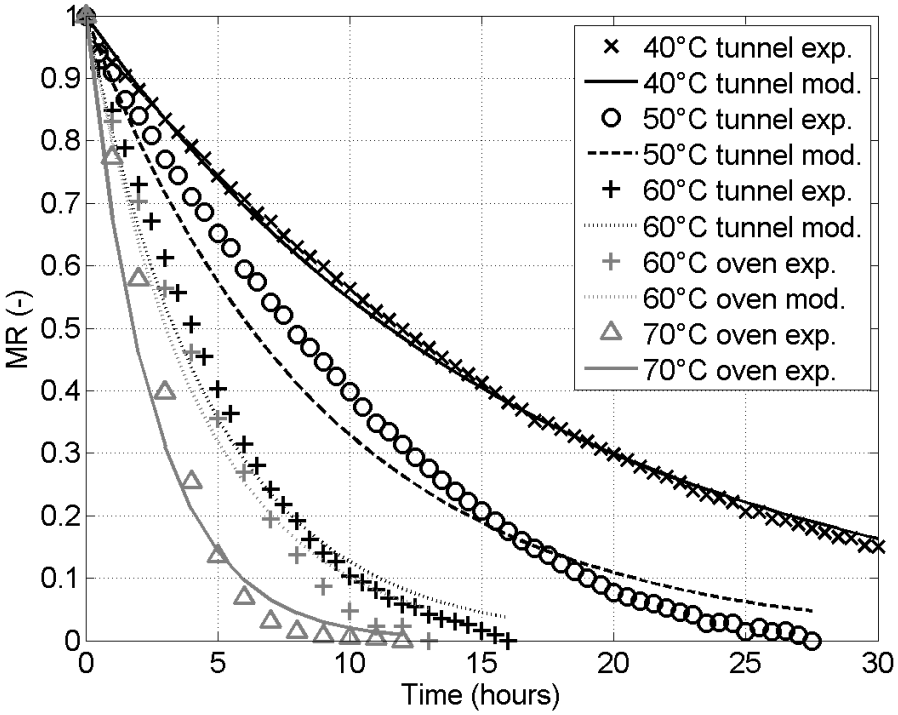

Figure A1. Moisture ratio MR_t as a function of time from experiments (symbols) and the Newton model (lines). Black symbols correspond to tests in the tunnel dryer while gray symbols correspond to tests in the oven dryer. Each symbol corresponds to a given drying temperature.

Appendix B. Page Model

On top of the Newton model and Henderson and Pabis model presented in the text, the Page thin layer models was also tested: [20]

$$MR = \exp(-kt^n) \tag{A1}$$

This model was fitted using linear regression applied on the logarithm of the logarithm of equation (A1):

$$\log(-\log(MR)) = \log(k) + n * \log(t) \tag{A2}$$

Optimal values of the parameters for the fitting of this model with the experimental data are summarized in Table A1. These results highlight that the Page model give optimal results that only slightly differ from the Newton or the Henderson and Pabis models. Indeed, the optimal k values differ of maximum 20% from the Newton model values. n value is in the range $0.947 < n < 1.2$ for all the tested conditions. These values stay close to $n = 1$ for which the Page model reduces to the Newton model. Compared to Newton and Henderson and Pabis models, the r^2 value is slightly increased, thanks to the second adjusted parameter. The $RMSE$ also increases showing a weaker prediction. This rise of the $RMSE$ can be attributed to the increased number of fitted parameters.

 doi:10.20944/preprints202405.1478.v1

Table A1. Identified values of k, n,a, c and the corresponding statistics for the three supplementary models at different temperatures.

Experiments	Parameter	Page
$40°C$ in tunnel	$k\ (h^{-1})$	4.1
	n	0.947
	r^2	0.998
	$RMSE$	0.034
$50°C$ in tunnel	$k\ (h^{-1})$	5.55
	n	0.998
	r^2	0.989
	$RMSE$	0.087
$60°C$ in tunnel	$k\ (h^{-1})$	11.0
	n	1.01
	r^2	0.992
	$RMSE$	0.069
$60°C$ in oven	$k\ (h^{-1})$	10.6
	n	1.09
	r^2	0.995
	$RMSE$	0.054
$70°C$ in oven	$k\ (h^{-1})$	15.03
	n	1.2
	r^2	0.996
	$RMSE$	0.049

Appendix C. Model of the Evolution of Volume Ratio and Porosity as a Function of the Moisture Ratio

At a given time t, the sample has a total volume V_t, equal to the sum of a volume of solid V_S, a volume of liquid V_L and a volume of gas V_G:

$$V_t = V_S + V_G + V_L \tag{A3}$$

Initially, this total volume is composed only of liquid and solid:

$$V_0 = V_{S0} + V_{L0} \tag{A4}$$

The volume of solid is assumed to be constant over time ($V_S = V_{S0}$). When the volume of liquid is reduced by the evaporation, we assume that it is replaced by gas, but that only a constant fraction α of the freed volume stays inside of the sample. Thus, the gas volume in the sample writes:

$$V_G = \alpha(V_{L0} - V_L). \tag{A5}$$

Combining equations (A3), (A4) and (A5) leads to:

$$\frac{V_t}{V_0} = 1 - (1 - \alpha)\frac{V_{L0} - V_L}{V_0}. \tag{A6}$$

By introducing the initial porosity defined as:

$$\epsilon_0 = \frac{V_{L0}}{V_0} \tag{A7}$$

and taking into account that:

 doi:10.20944/preprints202405.1478.v1

$$\frac{V_L}{V_0} = \frac{V_{L0}}{V_0}\frac{V_L}{V_{L0}} = \epsilon_0 \frac{X_t}{X_0} = \epsilon_0 MR \tag{A8}$$

equation (A9) becomes:

$$\frac{V_t}{V_0} = 1 - \epsilon_0(1-\alpha)(1-MR) \tag{A9}$$

The porosity at time t can then be defined as:

$$\epsilon_t = \frac{V_L + V_G}{V_t} \tag{A10}$$

By using equations (A9), (A7), and (A9), equation (A10) can be rewritten as:

$$\epsilon_t = \frac{V_L + \alpha(V_{L0} - V_L)}{V_0[1 - \epsilon_0(1-\alpha)(1-MR)]} = \epsilon_0 \frac{\alpha + (1-\alpha)MR}{1 - \epsilon_0(1-\alpha)(1-MR)} \tag{A11}$$

References

1. de Gier, S.; Verhoeckx, K. Insect (food) allergy and allergens. *Molecular Immunology* **2018**, *100*, 82–106. doi:10.1016/j.molimm.2018.03.015.
2. de Castro, R.J.S.; Ohara, A.; Aguilar, J.G.d.S.; Domingues, M.A.F. Nutritional, functional and biological properties of insect proteins: Processes for obtaining, consumption and future challenges. *Trends in Food Science & Technology* **2018**, *76*, 82–89. doi:10.1016/j.tifs.2018.04.006.
3. Gere, A.; Radványi, D.; Héberger, K. Which insect species can best be proposed for human consumption? *Innovative Food Science & Emerging Technologies* **2019**, *52*, 358–367. doi:10.1016/j.ifset.2019.01.016.
4. Hobbi, P.; Bekhit, A.E.D.A.; Debaste, F.; Lei, N.; Shavandi, A. Insect-Derived Protein as Food and Feed. In *Alternative Proteins*; CRC Press, 2022. Num Pages: 48.
5. Mancini, S.; Moruzzo, R.; Riccioli, F.; Paci, G. European consumers' readiness to adopt insects as food. A review. *Food Research International* **2019**, *122*, 661–678. doi:10.1016/j.foodres.2019.01.041.
6. Sun-Waterhouse, D.; Waterhouse, G.I.N.; You, L.; Zhang, J.; Liu, Y.; Ma, L.; Gao, J.; Dong, Y. Transforming insect biomass into consumer wellness foods: A review. *Food Research International* **2016**, *89*, 129–151. doi:10.1016/j.foodres.2016.10.001.
7. Akullo, J.; Obaa, B.; Acai, J.O.; Nakimbugwe, D.; Agea, J. Knowledge, attitudes and practices on edible insects in Lango sub-region, northern Uganda. *Journal of Insects as Food and Feed* **2017**, *3*, 73–81. Publisher: Wageningen Academic Publishers, doi:10.3920/JIFF2016.0033.
8. Kinyuru, J.N.; Kenji, G.M.; Njoroge, S.M.; Ayieko, M. Effect of Processing Methods on the In Vitro Protein Digestibility and Vitamin Content of Edible Winged Termite (Macrotermes subhylanus) and Grasshopper (Ruspolia differens). *Food and Bioprocess Technology* **2010**, *3*, 778–782. doi:10.1007/s11947-009-0264-1.
9. Kröncke, N.; Böschen, V.; Woyzichovski, J.; Demtröder, S.; Benning, R. Comparison of suitable drying processes for mealworms (Tenebrio molitor). *Innovative Food Science & Emerging Technologies* **2018**, *50*, 20–25. doi:10.1016/j.ifset.2018.10.009.
10. Niassy, S.; Fiaboe, K.; Affognon, H.; Akutse, K.; Tanga, M.; Ekesi, S. African indigenous knowledge on edible insects to guide research and policy. *Journal of Insects as Food and Feed* **2016**, *2*, 161–170. Publisher: Wageningen Academic Publishers, doi:10.3920/JIFF2015.0085.
11. Tiencheu, B.; Womeni, H.M.; Linder, M.; Mbiapo, F.T.; Villeneuve, P.; Fanni, J.; Parmentier, M. Changes of lipids in insect (Rhynchophorus phoenicis) during cooking and storage. *European Journal of Lipid Science and Technology* **2013**, *115*, 186–195. _eprint: https://onlinelibrary.wiley.com/doi/pdf/10.1002/ejlt.201200284, doi:10.1002/ejlt.201200284.
12. Lautenschläger, T.; Neinhuis, C.; Kikongo, E.; Henle, T.; Förster, A. Impact of different preparations on the nutritional value of the edible caterpillar Imbrasia epimethea from northern Angola. *European Food Research and Technology* **2017**, *243*, 769–778. doi:10.1007/s00217-016-2791-0.
13. Spreutels, L.; Debaste, F.; Legros, R.; Haut, B. Experimental characterization and modeling of Baker's yeast pellet drying. *Food Research International* **2013**, *52*, 275–287. doi:10.1016/j.foodres.2013.02.038.

14. Azzollini, D.; Derossi, A.; Severini, C. Understanding the drying kinetic and hygroscopic behaviour of larvae of yellow mealworm (Tenebrio molitor) and the effects on their quality. *Journal of Insects as Food and Feed* **2016**, *2*, 233–243. Publisher: Wageningen Academic Publishers, doi:10.3920/JIFF2016.0001.
15. Souza, L.F.d.; Andrade, E.T.d.; Rios, P.d.A. Determination of volumetric contraction and drying kinetics of the dryed banana. *Theoretical and Applied Engineering* **2019**, *3*, 20–30. Number: 1, doi:10.31422/taae.v2i4.10.
16. Oikonomopoulou, V.P.; Krokida, M.K. Novel Aspects of Formation of Food Structure during Drying. *Drying Technology* **2013**, *31*, 990–1007. Publisher: Taylor & Francis _eprint: https://doi.org/10.1080/07373937.2013.771186.
17. Essalhi, H.; Tadili, R.; Bargach, M.N. Conception of a Solar Air Collector for an Indirect Solar Dryer. Pear Drying Test. *Energy Procedia* **2017**, *141*, 29–33. doi:10.1016/j.egypro.2017.11.114.
18. Heilporn, C.; Haut, B.; Debaste, F.; van der Pol, F.; Boey, C.; Nonclercq, A. Implementation of a rational drying process for fish conservation. *Food Security* **2010**, *2*, 71–80. doi:10.1007/s12571-009-0049-4.
19. Gerard, P.; Mpawenayo, R.; Douzane, M.; Debaste, F. Influence of climatic conditions on evaporation in soil samples. *Environmental Geotechnics* **2019**, *6*, 323–333. Publisher: ICE Publishing, doi:10.1680/jenge.15.00069.
20. Gasa, S.; Sibanda, S.; Workneh, T.S.; Laing, M.; Kassim, A. Thin-layer modelling of sweet potato slices drying under naturally-ventilated warm air by solar-venturi dryer. *Heliyon* **2022**, *8*, e08949. https://doi.org/10.1016/j.heliyon.2022.e08949.
21. Crank, J. *The Mathematics of Diffusion*; Clarendon Press, 1979. Google-Books-ID: eHANhZwVouYC.
22. Erbay, Z.; Icier, F. A Review of Thin Layer Drying of Foods: Theory, Modeling, and Experimental Results. *Critical Reviews in Food Science and Nutrition* **2010**, *50*, 441–464. Publisher: Taylor & Francis _eprint: https://doi.org/10.1080/10408390802437063, doi:10.1080/10408390802437063.
23. Tshanga, C.B.; Malumba, P.; Mutiaka, B.K.; Bindelle, J.; Debaste, F. Dynamic vapour sorption isotherms and isosteric heats of sorption of two edible insects (Cirina forda and Rhyncophorus phoenicis). *Journal of Insects as Food and Feed* **2023**, *9*, 1017–1026. Publisher: Wageningen Academic Publishers, doi:10.3920/JIFF2022.0080.
24. Quirijns, E.J.; van Boxtel, A.J.; van Loon, W.K.; van Straten, G. Sorption isotherms, GAB parameters and isosteric heat of sorption. *Journal of the Science of Food and Agriculture* **2005**, *85*, 1805–1814. _eprint: https://onlinelibrary.wiley.com/doi/pdf/10.1002/jsfa.2140, doi:10.1002/jsfa.2140.
25. Farias, R.P.; Gomez, R.S.; Silva, W.P.; Silva, L.P.L.; Oliveira Neto, G.L.; Santos, I.B.; Carmo, J.E.F.; Nascimento, J.J.S.; Lima, A.G.B. Heat and Mass Transfer, and Volume Variations in Banana Slices during Convective Hot Air Drying: An Experimental Analysis. *Agriculture* **2020**, *10*, 423. Number: 10 Publisher: Multidisciplinary Digital Publishing Institute, doi:10.3390/agriculture10100423.
26. Ratti, C. Shrinkage during drying of foodstuffs. *Journal of Food Engineering* **1994**, *23*, 91–105. doi:10.1016/0260-8774(94)90125-2.